

A Measurement of R_c using the SLD Detector *

The SLD Collaboration **

*Stanford Linear Accelerator Center
Stanford University, Stanford, CA 94309*

Contact: Nicolo de Groot, nicolo@slac.stanford.edu

Abstract

We report a new measurement of R_c using data obtained with the SLD detector in 1993-1997. This measurement uses a double tag technique, where the selection of a c hemisphere is based on the reconstructed mass of the charm hadron decay vertex. The method uses the 3D vertexing capabilities of SLD's CCD vertex detectors and the small and stable SLC beams to obtain a high c -tagging efficiency and purity of 15% and 69%, respectively. We obtain a preliminary 93-97 result of $R_c = 0.1794 \pm 0.0085_{stat.} \pm 0.0061_{syst.}$.

Contributed to the XXIX International Conference on High Energy Physics, July 22 - July 29 1998, Vancouver, Canada

*Work supported by Department of Energy contract DE-AC03-76SF00515 (SLAC).

1 Introduction

A measurement of the fraction of hadronic Z^0 decays into charm quarks, $R_c = \Gamma_{Z^0 \rightarrow c\bar{c}}/\Gamma_{Z^0 \rightarrow had}$, is a valuable test of the electroweak theory of the SM. In this paper we present a preliminary measurement of R_c with the SLD detector using a new, self-calibrating, double-tag method. The systematic uncertainties for this method are small and mostly uncorrelated with the errors from semi-leptonic or charm counting measurements of R_c .

A previous measurement of R_b by SLD introduced the mass tag [1] to identify B hadrons with high efficiency and purity. This same mass tag is used in this analysis of R_c . Both the 1993-1995 period, with the old VXD2 detector, and the 1996-1997 SLD run with the upgraded vertex detector VXD3 [2] have been analyzed. This measurement is an update of a previously presented result on our 1993-1996 dataset [3]. A total of 300k Z^0 events were used in this analysis. A detailed description of the SLD detector can be found elsewhere [4].

2 Method

Hadronic events are divided into two hemispheres by the plane perpendicular to the thrust axis of the event. Each hemisphere is then individually tagged for the presence of a B hadron (b -tag) or a D hadron (c -tag). The b tag has relatively little contamination from charm and uds , the c tag selects a mixture of b and c with little uds background. The fraction of hemispheres tagged as originating from b quarks is given by

$$F_s = R_b\epsilon_b + R_c\epsilon_c + (1 - R_c - R_b)\epsilon_{uds}$$

and the fraction of events with both hemispheres tagged as originating from a b quark is given by

$$F_d = R_b(\epsilon_b^2 + \lambda_b^h(\epsilon_b - \epsilon_b^2)) + R_c(\epsilon_c^2 + \lambda_c^h(\epsilon_c - \epsilon_c^2)) + (1 - R_c - R_b)\epsilon_{uds}^2$$

The above two equations are solved for R_b and the efficiency for tagging a B hadron, ϵ_b . The efficiencies for tagging charm, ϵ_c , and uds , ϵ_{uds} , as well as the bottom and charm correlations for tagging both hemispheres in an event, λ_b^h and λ_c^h , respectively, are taken from Monte Carlo (MC) studies. The fraction of hemispheres tagged by the c -tag is:

$$G_s = R_b\eta_b + R_c\eta_c + (1 - R_c - R_b)\eta_{uds}$$

and the fraction of events with both hemispheres tagged with a c -tag.

$$G_d = R_b(\eta_b^2 + \lambda_b^l(\eta_b - \eta_b^2)) + R_c(\eta_c^2 + \lambda_c^l(\eta_c - \eta_c^2)) + (1 - R_c - R_b)\eta_{uds}^2$$

In addition we have the fraction of events with a b tag on one side and a c tag on the other side.

$$M = R_b\epsilon_b\eta_b + R_c\epsilon_c\eta_c + (1 - R_c - R_b)\epsilon_{uds}\eta_{uds}$$

For the last 3 equations, the uds efficiency (η_{uds}) and the correlations are again taken from Monte Carlo. $R - c$ and ϵ_b are known from the first two equations and we are left with 3 equations with three unknowns. This gives us a determination of R_c and η_c from the data.

3 Event Selection

Hadronic event selection is based on the visible energy and track multiplicity in the event. The visible energy is measured using central drift chamber (CDC) tracks and must exceed 18GeV. There must be at least 7 CDC tracks, 3 of which are reconstructed with hits in the vertex detector, We also require that the thrust axis, measured from calorimeter clusters, satisfies $|\cos\theta| < 0.75$. This insures that the event is well contained within the acceptance of the vertex detector. All detector elements are also required to be fully operational. Additionally, we restrict events to 3 jets or less to make sure that we have well defined hemispheres. Jets being defined by the JADE algorithm [5] with a $y_{cut} = 0.02$ A total of 66K events pass the above hadronic event selection and jet cuts in the 1997 data. Background, predominately due to taus, is estimated at $< 0.1\%$.

The SLC interaction point (IP) has a size of approximately $(1.5 \times 0.5 \times 700)\mu m$ in (x,y,z) . The motion of the IP xy position over a short time interval is estimated to be $7\mu m$. Since this motion is smaller than the xy resolution for fitting tracks to find the primary vertex (PV) in a given event, we use the average IP position, $\langle IP \rangle$, for the x and y coordinates of the primary vertex. The average is obtained from tracks with hits in the vertex detector in 30 sequential hadronic events. The z coordinate of the PV is determine from each event separately. This results in a PV uncertainty of $7\mu m$ transverse and $20\mu m$ longitudinally to the beam direction. By averaging over many hadronic events to find the primary vertex xy , we are able to reduce significantly the systematic error introduced from the PV uncertainty.

3.1 Track Selection

Reconstruction of the mass of heavy hadrons is preceded by first identifying secondary vertices in each hemisphere. Only tracks that are well measured are included in the vertex and mass reconstruction. Tracks are required to have at least 23 CDC hits and start within a radius of 50cm of the IP. The CDC track is also required to extrapolate to within 1cm of the IP in xy and within 1.5cm of the PV in z . We require two hits in the vertex detector, VXD3. The combined drift chamber + vertex detector fit must satisfy $\chi^2/d.o.f. < 8$ $|\cos\theta| < 0.87$. Tracks with an xy impact parameter $> 3.0\text{mm}$ or an xy impact parameter error $> 250\mu m$ with respect to the IP are removed from consideration in the vertex and mass reconstruction.

3.2 Vertex Mass Reconstruction

Secondary vertex identification is done using a topological vertexing method [6]. This method searches for space points in 3D where track density functions have a maximum. Each track is parameterized by a Gaussian density tube with a width equal to the uncertainty in the measured track position at the IP. Points in space where there is a large overlap of Gaussian probability tubes is considered as a possible vertex point. By clustering maxima in the

overlap density distribution, secondary vertices are found for the two hemispheres. We find secondary vertices in approximately 65% of all b hemispheres, 20% for charm, and less than 1% for uds hemispheres.

Only vertices that are significantly displaced from the PV are considered to be possible B or D hadron decay vertices. The distance between the PV and the secondary vertex is required to be at least 4σ .

Due to the cascade nature of the B decay, tracks from the decay may not all originate from the same space point. This creates a problem if we want to accurately reconstruct the invariant mass of the B hadron decay vertex. Therefore, a process of adding tracks to the secondary vertex has been developed to pick up these tracks. A track is attached to the secondary vertex if

- the impact parameter, T , to the PV-secondary vertex axis, is $< 1mm$,
- the distance, L , along the axis to this point, is $> 0.5mm$, and
- $L/D > 0.25$, where D is the secondary vertex decay distance.

The first cut ensures that the added track is close to the secondary vertex. The second and third cuts prevent the addition of tracks that are consistent with coming from the IP.

The mass of the secondary vertex is calculated using the tracks that are associated with the vertex. These include the tracks that have been added using the above procedure. Each track is assigned the mass of the charged pion and the invariant mass of the vertex is then calculated. The reconstructed mass is corrected to account for neutral particles. Using kinematic information from the vertex flight path and the momentum sum of the tracks associated with the secondary vertex, we add a minimum amount of missing momentum to the invariant mass. This is done by assuming the true B hadron momentum is in a direction along the vertex flight path, and taking the errors on the IP and secondary vertex into account. This p_t corrected mass is given by

$$M_c = \sqrt{M_{tk}^2 + P_t^2} + |P_t|$$

where M_{tk} is the reconstructed mass for the tracks associated with the secondary vertex. We restrict the contribution to the invariant mass that the additional transverse momentum adds to be less than the initial mass of the secondary vertex. This cut ensures that poorly measured vertices in uds events do not leak into the sample by adding in large P_t . Monte Carlo and data comparisons for the P_t corrected mass (M_c) distributions can be seen in figure 1.

3.3 Flavor Tag

A bottom tag is defined as a hemisphere with an invariant mass above 2 GeV. The intermediate mass region, between 0.55 and 2 GeV contains a mixture of b and c , with a small uds

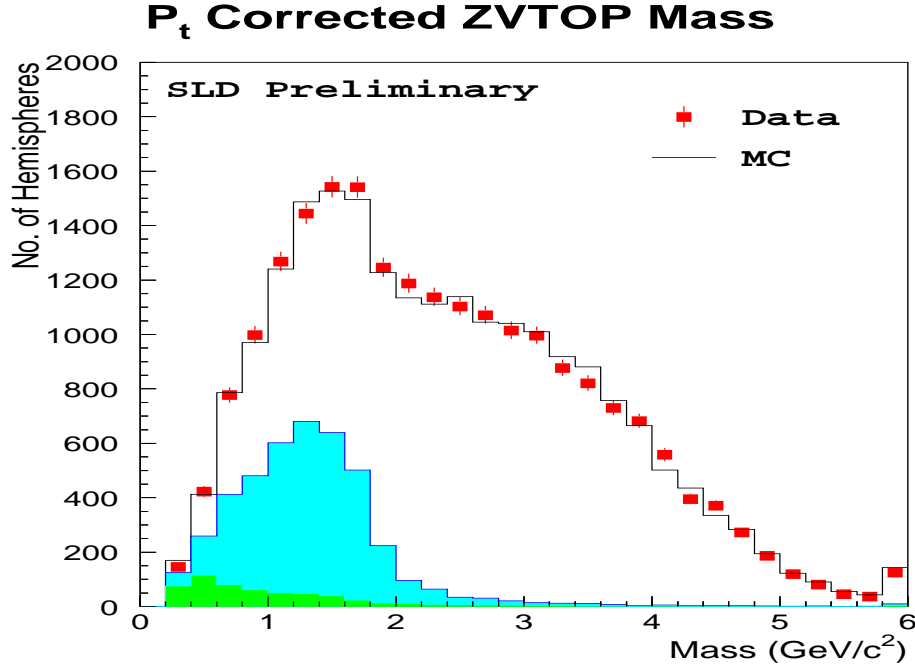


Figure 1: Vertex mass corrected for missing p_t for data and MC. The dark shaded area are the uds events, the light shaded area c events and the white area the b events.

background. We define some additional cuts to reject b and uds . A charm tag is defined as follows:

- $0.55 < M_c < 2\text{GeV}$
- Vertex momentum (P_V) greater than 5 GeV.
- Fragmentation cut: $15M_c - P_V < 10$. This uses the fact that D hadrons from charm have a higher momentum for the same mass than those from b quarks. The effect of this cut can be seen in fig. 2.

4 Results

For 1997 the measured efficiency is $\eta_c = 15.4 \pm 1.3\%$ for charm events, with a purity of $\pi_c = 69 \pm 2\%$, again in agreement with the Monte Carlo values of $\eta_c^{MC} = 15.2\%$ and $\pi_c^{MC} = 69\%$. The efficiency for the tag is $\epsilon_b = 0.499$ at a purity of 0.98. The background is made up of 3% uds and 28% b . The Monte Carlo sample was made up of 529k generic $q\bar{q}$, 418k $b\bar{b}$ and 198k $c\bar{c}$. The correlations are: $\lambda_c^l = -0.00002$, $\lambda_b^l = -0.0078$ and $\lambda_b^h = 0.0010$. The R_c value extracted from 66k selected events in 1997 is:

$$R_c = 0.1785 \pm 0.0118$$

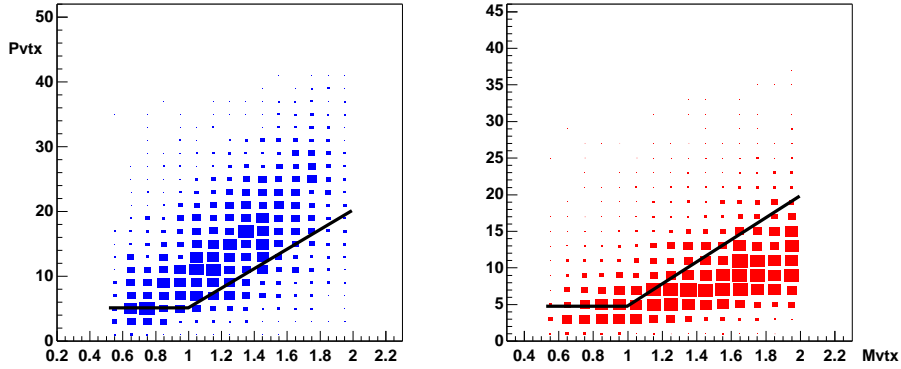


Figure 2: Vertex momentum as a function of vertex mass for c (left) and b (right) events

Combined with our 1993-1996 results[3] this gives us an average of:

$$R_c = 0.1794 \pm 0.0085$$

5 Systematic Errors

The systematic uncertainty in measuring R_c is due to a combination of MC and detector related quantities. Each contribution to the error manifests itself through the uds efficiency and charm and bottom correlations. The systematic errors are given in table 1 and described below.

5.1 Detector Systematic Error

The Monte Carlo contains slightly more reconstructed tracks than the data. Therefore, tracks are randomly removed from the MC depending on the transverse momentum, p_t , ϕ , and $\cos\theta$ of the track, so that the multiplicity in the data and MC for all hadronic events agree. The systematic error due to this efficiency correction is obtained by assigning an error equal to the change in R_c when the analysis is done with and without the corrections.

Similarly, the impact parameter resolution of MC tracks is better than data tracks. Therefore, the impact parameters in the MC are smeared so that the distributions agree well with the data distributions. For the 1997 analysis we apply a smearing of $9\mu m$ in rz . The full difference in R_c introduced by the smearing process is estimated as the systematic error.

Simulation errors which affect the tagging efficiency are studied by comparing data and MC ϕ and $\cos\theta$ distributions of the c -tagging rates, and a systematic error is assigned to the difference. Finally the event selection introduces a small bias in R_c and R_b . We take the full effect as a systematic error.

Source	δR_c
MC statistics	0.0013
Detector Effects	
resolution smearing	0.0013
event selection, 100%	0.0005
track efficiency	0.0017
tag $\cos \theta$ variation	0.0012
Physics effects	
charm systematics	0.0016
b systematics	0.0004
IP correlation	0.0036
$g \rightarrow b\bar{b}, c\bar{c}$:	0.0015
hard <i>gluon</i> radiation	0.0015
uds background, 25%	0.0030
total	0.0061

Table 1: Systematic errors on R_c for the 93-95 and 96 data

5.2 Physics Systematic Error

Since the efficiencies for b and c quarks are obtained from data we expect the systematic errors from b and c physics effects to come only through the hemisphere correlations and to be small. We vary the production rates, lifetimes and decay multiplicities according to the recommendations of the LEP Electroweak Working Group[8].

The two significant sources of systematic errors from light quark events come from the uncertainties in long lived strange particle production and gluon splitting into heavy quark pairs.

The uncertainty in the charm-tag efficiency for u , d and s is estimated from a light flavor tag. We require a charm tag on one side and no tag, with no track significantly away from the IP, on the other side. The difference in tagging rate between data and Monte Carlo is assumed to be caused by the light flavors only. From this we estimate the uncertainty in the uds fraction to be less than 25%. This difference is used to estimate the systematic error in R_c from light flavor background.

For gluon splitting effects, the $g \rightarrow b\bar{b}$ and $g \rightarrow c\bar{c}$ production rates are varied according to the OPAL $g \rightarrow c\bar{c}$ measurement [7] and the theoretical prediction for the ratio of $g \rightarrow b\bar{b}/g \rightarrow c\bar{c}$ [8].

Hard gluon radiation effects are estimated from $\pm 30\%$ variation of the fraction of MC events where both B or D hadrons are contained within the same hemisphere and a hard gluon is in the other.

One important correlation between the two hemispheres is through the primary vertex. We take the difference between R_c measured with the reconstructed IP and R_c measured with a Monte Carlo event true IP as a preliminary estimate of the systematic uncertainty coming from IP correlations.

This leads us to the following preliminary result for 97:

$$R_c = 0.1776 \pm 0.0119 \pm 0.0055$$

Combining it with our 1993-1996 result[3] gives our preliminary 93-97 result:

$$R_c = 0.1794 \pm 0.0085 \pm 0.0061$$

This number includes a correction for the event selection bias and the photon exchange interference.

6 Conclusions

We have updated our measurement of R_c using a double tag method that uses some of the unique features of the SLD detector. Our updated result based on 350K hadronic Z^0 is

$$R_c = 0.1794 \pm 0.0085 \pm 0.0061 \quad \text{SLD 93-97 Preliminary}$$

This result is still statistically limited and agrees with the SM expectation of 0.172. The statistical error is comparable to most of the LEP measurements and the systematic errors are small and mostly uncorrelated with those from existing methods.

References

- [1] K. Abe *et al.*, Phys. Rev. Lett. 80, 660 (1997).
- [2] K. Abe *et al.*, Nucl. Inst. Meth. **A400**, 287, (1997).
- [3] K. Abe *et al.*, SLAC-PUB-7594, submitted to Lepton-Photon 1997.
- [4] K. Abe *et al.* Phys Rev. **D53**, 1023, (1996).
- [5] W. Bartel *et al.*, Z. Phys. **C33**, 23 (1986).
- [6] D. Jackson, Nucl. Instr. Meth. **A388**, 247 (1997).
- [7] OPAL Collab. R. Akers *et al.*, Phys. Lett. **B353**, 595, (1995).
- [8] The Lep Electroweak Working Group, *LEPHF/97-01* July 1997.

Acknowledgements

This work was supported by Department of Energy contracts: DE-FG02-91ER40676 (BU), DE-FG03-92ER40701 (CIT), DE-FG03-91ER40618 (UCSB), DE-FG03-92ER40689 (UCSC), DE-FG03-93ER40788 (CSU), DE-FG02-91ER40672 (Colorado), DE-FG02-91ER40677 (Illinois), DE-AC03-76SF00098 (LBL), DE-FG02-92ER40715 (Massachusetts), DE-AC02-76ER03069 (MIT), DE-FG06-85ER40224 (Oregon), DE-AC03-76SF00515 (SLAC), DE-FG05-91ER40627 (Tennessee), DE-AC02-76ER00881 (Wisconsin), DE-FG02-92ER40704 (Yale); National Science Foundation grants: PHY-91-13428 (UCSC), PHY-89-21320 (Columbia), PHY-92-04239 (Cincinnati), PHY-88-17930 (Rutgers), PHY-88-19316 (Vanderbilt), PHY-92-03212 (Washington); the UK Science and Engineering Research Council (Brunel and RAL); the Istituto Nazionale di Fisica Nucleare of Italy (Bologna, Ferrara, Frascati, Pisa, Padova, Perugia); and the Japan-US Cooperative Research Project on High Energy Physics (Nagoya, Tohoku).

** List of Authors

K. Abe,⁽¹⁹⁾ K. Abe,⁽²⁹⁾ T. Abe,⁽²⁷⁾ I. Adam,⁽²⁷⁾ H. Akimodo,⁽²⁷⁾ N. Allen,⁽⁴⁾ W.W. Ash,⁽²⁷⁾ D. Aston,⁽²⁷⁾ K.G. Baird,⁽¹⁶⁾ C. Baltay,⁽³³⁾ H.R. Band,⁽³²⁾ M.B. Barakat,⁽³³⁾ O. Bardou,⁽¹⁶⁾ T. Barklow,⁽²⁷⁾ J.M. Bauer,⁽¹⁸⁾ A.O. Bazarko,⁽¹¹⁾ G. Bellodi,⁽³⁶⁾ R. Ben-David,⁽³³⁾ A.C. Benvenuti,⁽²⁾ G.M. Bilei,⁽²²⁾ D. Bisello,⁽²¹⁾ G. Blaylock,⁽⁷⁾ J.R. Bogart,⁽²⁷⁾ B. Bolen,⁽¹⁷⁾ T. Bolton,⁽¹¹⁾ G.R. Bower,⁽²⁷⁾ J.E. Brau,⁽²⁰⁾ M. Breidenbach,⁽²⁷⁾ W.M. Bugg,⁽²⁸⁾ D. Burke,⁽²⁷⁾ T.H. Burnett,⁽³¹⁾ P.N. Burrows,⁽³⁶⁾ W. Busza,⁽¹⁶⁾ A. Calcaterra,⁽¹³⁾ D.O. Caldwell,⁽⁶⁾ D. Calloway,⁽²⁷⁾ B. Camanzi,⁽¹²⁾ M. Carpinelli,⁽²³⁾ R. Cassell,⁽²⁷⁾ R. Castaldi,⁽²³⁾ A. Castro,⁽²¹⁾ M. Cavalli-Sforza,⁽⁷⁾ A. Chou,⁽²⁷⁾ E. Church,⁽³¹⁾ H.O. Cohn,⁽²⁸⁾ J.A. Coller,⁽³⁾ V. Cook,⁽³¹⁾ R. Cotton,⁽⁴⁾ R.F. Cowan,⁽¹⁶⁾ D.G. Coyne,⁽⁷⁾ G. Crawford,⁽²⁷⁾ A. D'Oliveira,⁽⁸⁾ C.J.S. Damerell,⁽²⁵⁾ M. Daoudi,⁽²⁷⁾ S. Dasu,⁽²⁷⁾ N. De Groot,⁽²⁷⁾ R. De Sangro,⁽¹³⁾ R. Dell'Orso,⁽²³⁾ M. Dima,⁽⁹⁾ P. Dervan,⁽⁴⁾ D.N. Dong,⁽¹⁶⁾ P.Y.C. Du,⁽²⁸⁾ R. Dubois,⁽²⁷⁾ B.I. Eisenstein,⁽¹⁴⁾ V. O. Eschenburg,⁽¹⁸⁾ E. Etzion,⁽³²⁾ S. Fahey,⁽¹⁰⁾ D. Falciari,⁽²²⁾ C. Fan,⁽¹⁰⁾ M.J. Fero,⁽¹⁶⁾ K. Flood,⁽¹⁷⁾ R. Frey,⁽²⁰⁾ T. Gillman,⁽²⁵⁾ G. Gladding,⁽¹⁴⁾ S. Gonzalez,⁽¹⁶⁾ E.L. Hart,⁽²⁸⁾ J.L. Harton,⁽⁹⁾ A. Hasan,⁽⁴⁾ Y. Hasegawa,⁽²⁹⁾ K. Hasuko,⁽²⁹⁾ S. Hedges,⁽⁴⁾ S.S. Hertzbach,⁽¹⁷⁾ M.D. Hildreth,⁽²⁷⁾ J. Huber,⁽²⁰⁾ M.E. Huffer,⁽²⁷⁾ E.W. Hughes,⁽²⁷⁾ X. Huynh,⁽²⁷⁾ H. Hwang,⁽²⁰⁾ M. Iwasaki,⁽²⁰⁾ Y. Iwasaki,⁽²⁹⁾ D. Jackson,⁽²⁵⁾ P. Jacques,⁽²⁴⁾ J. Jaros,⁽²⁷⁾ A.S. Johnson,⁽³⁾ J.R. Johnson,⁽³²⁾ R.A. Johnson,⁽⁸⁾ T. Junk,⁽²⁷⁾ R. Kajikawa,⁽¹⁹⁾ M. Kalelkar,⁽²⁴⁾ Y. Kamyshkov,⁽²⁸⁾ H.J. Kang,⁽³⁴⁾ I. Karliner,⁽¹⁴⁾ H. Kawahara,⁽²⁷⁾ H.W. Kendall,⁽¹⁶⁾ Y. Kim,⁽²⁶⁾ M.E. King,⁽²⁷⁾ R. King,⁽²⁷⁾ R.R. Kofler,⁽¹⁷⁾ N.M. Krishna,⁽¹⁰⁾ R.S. Kroeger,⁽¹⁸⁾ J.F. Labs,⁽²⁷⁾ M. Langston,⁽²⁰⁾ A. Lath,⁽¹⁶⁾ J.A. Lauber,⁽¹⁰⁾ D.W.G. Leith,⁽²⁷⁾ V. Lia,⁽¹⁶⁾ C.J. Lin,⁽¹⁷⁾ X. Liu,⁽⁷⁾ M. Loreti,⁽²¹⁾ A. Lu,⁽⁶⁾ H.L. Lynch,⁽²⁷⁾ J. Ma,⁽³¹⁾ G. Mancinelli,⁽²⁴⁾ S. Manly,⁽³³⁾ G. Mantovani,⁽²²⁾ T.W. Markiewicz,⁽²⁷⁾ T. Maruyama,⁽²⁷⁾ H. Masuda,⁽²⁷⁾ E. Mazzucato,⁽¹²⁾ A.K. McKemey,⁽⁴⁾ B.T. Meadows,⁽⁸⁾ G. Menegatti,⁽¹²⁾ R. Messner,⁽²⁷⁾ P.M. Mockett,⁽³¹⁾ K.C. Moffeit,⁽²⁷⁾ T. Moore,⁽³³⁾ D. Muller,⁽²⁷⁾ T. Nagamine,⁽²⁷⁾ S. Narita,⁽²⁹⁾ U. Nauenberg,⁽¹⁰⁾ H. Neal,⁽²⁷⁾ M. Nussbaum,⁽⁸⁾ Y. Ohnishi,⁽¹⁹⁾ N. Oishi,⁽¹⁹⁾

D. Onoprienko,⁽²⁸⁾ L.S. Osborne,⁽¹⁶⁾ R.S. Panvini,⁽³⁰⁾ H. Park,⁽²⁰⁾ C.H. Park,⁽³⁵⁾
 T.J. Pavel,⁽²⁷⁾ I. Peruzzi,⁽¹³⁾ M. Piccolo,⁽¹³⁾ L. Piemontese,⁽¹²⁾ E. Pieroni,⁽²³⁾ K.T. Pitts,⁽²⁰⁾
 R.J. Plano,⁽²⁴⁾ R. Prepost,⁽³²⁾ C.Y. Prescott,⁽²⁷⁾ G.D. Punkar,⁽²⁷⁾ J. Quigley,⁽¹⁶⁾
 B.N. Ratcliff,⁽²⁷⁾ T.W. Reeves,⁽³⁰⁾ J. Reidy,⁽¹⁸⁾ P.L. Reinertsen,⁽⁷⁾ P.E. Rensing,⁽²⁷⁾
 L.S. Rochester,⁽²⁷⁾ P.C. Rowson,⁽¹¹⁾ J.J. Russell,⁽²⁷⁾ O.H. Saxton,⁽²⁷⁾ T. Schalk,⁽⁷⁾
 R.H. Schindler,⁽²⁷⁾ U. Schneekloth,⁽¹⁶⁾ B.A. Schumm,⁽¹⁵⁾ J. Schwiening,⁽²⁷⁾ S. Sen,⁽³³⁾
 V.V. Serbo,⁽²⁷⁾ M.H. Shaevitz,⁽¹¹⁾ J.T. Shank,⁽³⁾ G. Shapiro,⁽¹⁵⁾ D.J. Sherden,⁽²⁷⁾
 K.D. Shmakov,⁽²⁸⁾ C. Simopoulos,⁽²⁷⁾ N.B. Sinev,⁽²⁰⁾ S.R. Smith,⁽²⁷⁾ M.B. Smy,⁽⁹⁾
 J.A. Snyder,⁽³³⁾ H. Staengle,⁽⁹⁾ P. Stamer,⁽²⁴⁾ H. Steiner,⁽¹⁵⁾ R. Steiner,⁽¹⁾ M.G. Strauss,⁽¹⁷⁾
 D. Su,⁽²⁷⁾ F. Suekane,⁽²⁹⁾ A. Sugiyama,⁽¹⁹⁾ S. Suzuki,⁽¹⁹⁾ M. Swartz,⁽²⁷⁾ A. Szumilo,⁽³¹⁾
 T. Takahashi,⁽²⁷⁾ F.E. Taylor,⁽¹⁶⁾ E. Torrence,⁽¹⁶⁾ J. Thom,⁽²⁷⁾ A.I. Trandafir,⁽¹⁷⁾
 J.D. Turk,⁽³³⁾ T. Usher,⁽²⁷⁾ C. Vannini,^(xx) J. Va'vra,⁽²⁷⁾ C. Vannini,⁽²³⁾ E. Vella,⁽²⁷⁾
 J.P. Venuti,⁽³⁰⁾ R. Verdier,⁽¹⁶⁾ P.G. Verdini,⁽²³⁾ S.R. Wagner,⁽²⁷⁾ D.L. Wagner,⁽¹⁰⁾
 A.P. Waite,⁽²⁷⁾ J. Wang,⁽²⁷⁾ C. Ward,⁽⁴⁾ S.J. Watts,⁽⁴⁾ A.W. Weidemann,⁽²⁸⁾ E.R. Weiss,⁽³¹⁾
 J.S. Whitaker,⁽³⁾ S.L. White,⁽²⁸⁾ F.J. Wickens,⁽²⁵⁾ D.C. Williams,⁽¹⁶⁾ S.H. Williams,⁽²⁷⁾
 S. Willocq,⁽²⁷⁾ R.J. Wilson,⁽⁹⁾ W.J. Wisniewski,⁽⁵⁾ M. Woods,⁽²⁷⁾ G.B. Word,⁽²⁴⁾
 T.R. Wright,⁽³²⁾ J. Wyss,⁽²¹⁾ R.K. Yamamoto,⁽¹⁶⁾ J.M. Yamartino,⁽¹⁶⁾ X. Yang,⁽²⁰⁾
 J. Yashima,⁽²⁹⁾ S.J. Yellin,⁽⁶⁾ C.C. Young,⁽²⁷⁾ H. Yuta,⁽²⁹⁾ G. Zapalac,⁽³²⁾ R.W. Zdarko,⁽²⁷⁾
 and J. Zhou⁽²⁰⁾

⁽¹⁾ Adelphi University, Garden City, New York 11530

⁽²⁾ INFN Sezione di Bologna, I-40126 Bologna, Italy

⁽³⁾ Boston University, Boston, Massachusetts 02215

⁽⁴⁾ Brunel University, Uxbridge, Middlesex UB8 3PH, United Kingdom

⁽⁵⁾ California Institute of Technology, Pasadena, California 91125

⁽⁶⁾ University of California at Santa Barbara, Santa Barbara, California 93106

⁽⁷⁾ University of California at Santa Cruz, Santa Cruz, California 95064

⁽⁸⁾ University of Cincinnati, Cincinnati, Ohio 45221

⁽⁹⁾ Colorado State University, Fort Collins, Colorado 80523

⁽¹⁰⁾ University of Colorado, Boulder, Colorado 80309

⁽¹¹⁾ Columbia University, New York, New York 10027

⁽¹²⁾ INFN Sezione di Ferrara and Università di Ferrara, I-44100 Ferrara, Italy

⁽¹³⁾ INFN Lab. Nazionali di Frascati, I-00044 Frascati, Italy

⁽¹⁴⁾ University of Illinois, Urbana, Illinois 61801

⁽¹⁵⁾ Lawrence Berkeley Laboratory, University of California, Berkeley, California 94720

⁽¹⁶⁾ Massachusetts Institute of Technology, Cambridge, Massachusetts 02139

⁽¹⁷⁾ University of Massachusetts, Amherst, Massachusetts 01003

⁽¹⁸⁾ University of Mississippi, University, Mississippi 38677

⁽¹⁹⁾ Nagoya University, Chikusa-ku, Nagoya 464 Japan

⁽²⁰⁾ University of Oregon, Eugene, Oregon 97403

⁽²¹⁾ INFN Sezione di Padova and Università di Padova, I-35100 Padova, Italy

⁽²²⁾ INFN Sezione di Perugia and Università di Perugia, I-06100 Perugia, Italy

⁽²³⁾ INFN Sezione di Pisa and Università di Pisa, I-56100 Pisa, Italy

- (²⁴) Rutgers University, Piscataway, New Jersey 08855
- (²⁵) Rutherford Appleton Laboratory, Chilton, Didcot, Oxon OX11 0QX United Kingdom
 - (²⁶) Sogang University, Seoul, Korea
- (²⁷) Stanford Linear Accelerator Center, Stanford University, Stanford, California 94309
 - (²⁸) University of Tennessee, Knoxville, Tennessee 37996
 - (²⁹) Tohoku University, Sendai 980 Japan
 - (³⁰) Vanderbilt University, Nashville, Tennessee 37235
 - (³¹) University of Washington, Seattle, Washington 98195
 - (³²) University of Wisconsin, Madison, Wisconsin 53706
 - (³³) Yale University, New Haven, Connecticut 06511
 - (³⁴) Sogang University, Seoul, Korea
 - (³⁵) Soongsil University, Seoul, Korea
 - (³⁶) Oxford University, Oxford OX1 3RH, United Kingdom